

# The Nature of Surface Barriers on Nanoporous Solids Explored by Microimaging of Transient Guest Distributions

Florian Hibbe,<sup>†</sup> Christian Chmelik,<sup>†</sup> Lars Heinke,<sup>†,‡</sup> Sanhita Pramanik,<sup>§</sup> Jing Li,<sup>§</sup> Douglas M. Ruthven,<sup>⊥</sup> Despina Tzoulaki,<sup>†,||</sup> and Jörg Kärger<sup>\*,†</sup>

<sup>†</sup>Faculty of Physics and Geosciences, Department of Interface Physics, University of Leipzig, Linnéstrasse 5, 04103 Leipzig, Germany

<sup>‡</sup>Fritz-Haber-Institute of the Max-Planck-Society, Faradayweg 4-6, 14195 Berlin, Germany

<sup>§</sup>Department of Chemistry and Chemical Biology, Rutgers University, 610 Taylor Road, Piscataway, New Jersey 08854, United States

<sup>⊥</sup>Department of Chemical Engineering, University of Maine, Orono, Maine 04469, United States

<sup>||</sup>Technical University of Munich, Faculty of Chemistry, Lichtenbergstrasse 4, 85748 Garching, Germany

**S** Supporting Information

**ABSTRACT:** Nanoporous solids are attractive materials for energetically efficient and environmentally friendly catalytic and adsorption separation processes. Although the performance of such materials is largely dependent on their molecular transport properties, our fundamental understanding of these phenomena is far from complete. This is particularly true for the mechanisms that control the penetration rate through the outer surface of these materials (commonly referred to as surface barriers). Recent detailed sorption rate measurements with Zn(tbip) crystals have greatly enhanced our basic understanding of such processes. Surface resistance in this material has been shown to arise from the complete blockage of most of the pore entrances on the outer surface, while the transport resistance of the remaining open pores is negligibly small. More generally, the revealed correlation between intracrystalline diffusion and surface permeation provides a new view of the nature of transport resistances in nanoporous materials acting in addition to the diffusion resistance of the regular pore network, leading to a rational explanation of the discrepancy which is often observed between microscopic and macroscopic diffusion measurements.

Diffusion, which involves the irregular movement of particles (atoms and molecules), is among the most fundamental and omnipresent phenomena in nature. It is the basis for many technologies,<sup>1</sup> particularly processes for separation and chemical conversion using nanoporous solids as adsorbents and catalysts. In such processes, the production rate cannot exceed the limits imposed by intraparticle diffusion. Diffusion studies reveal that nanoporous materials commonly deviate from their ideal textbook structure, with structural defects<sup>2,3</sup> often acting as transport resistances.<sup>4–9</sup> Lattice instability is particularly pronounced close to the crystal surface, and this facilitates the formation of defects. Transport resistances at a crystal surface (surface barriers) are a special case of the transport resistances that may appear quite generally at phase boundaries and the boundaries of compartments such as cell membranes.<sup>10</sup> The application of interference microscopy (IFM) and IR microscopy (IRM),<sup>11</sup> allows direct

measurement of these resistances. The experimental data so far accessible,<sup>12–14</sup> however, did not provide any insight into the nature of these resistances other than their magnitude. With the advent of the new MOF material, Zn(tbip)<sup>15</sup> (H2tbip = 5-*tert*-butyl isophthalic acid, Supporting Figure 1), this deficiency has now been overcome.

Conventionally, transport resistances at the boundary of nanoporous particles (and between different phases, in general) are considered as a thin layer (of thickness  $l$ ) of dramatically reduced diffusivity ( $D_{\text{barr}}$ ). Such a reduction may be explained by changes in the lattice properties close to the surface.<sup>16–18</sup> The magnitude of the resistance is characterized by the surface permeability,  $\alpha$ , defined by the relation<sup>19</sup>

$$j(x=0) = \alpha(c_{\text{eq}} - c(x=0)) \quad (1)$$

as the factor of proportionality between the flux  $j(x=0) = j_{\text{surf}}$  through the surface and the difference between the actual boundary concentration ( $c(x=0) = c_{\text{surf}}$ ) and the concentration  $c_{\text{eq}}$  established in equilibrium with the external gas pressure. According to Fick's first law,<sup>4</sup> molecular fluxes are the product of concentration gradient and diffusivity. With Figure 1, one thus obtains

$$j = D_{\text{barr}} \frac{c_{\text{eq}} - c(x=0)}{l} \quad (2)$$

and comparison with eq 1 yields

$$\alpha = D_{\text{barr}}/l \quad (3)$$

Alternatively, and completely equivalently with the model of Figure 1, transport inhibition may also result from a dramatic reduction of guest solubility. Then  $D_{\text{barr}}$  is replaced by the bulk diffusivity reduced by the ratio of the concentrations in the bulk and in the layer at equilibrium. In this model, diffusion ( $D$ ) and surface permeation ( $\alpha = D_{\text{barr}}/l$ ) are controlled by different mechanisms and vary independently of each other. Exactly this result was the outcome of all previous studies.<sup>12–14</sup> It was therefore a complete surprise to find that the concentration dependences of the intraparticle diffusivities<sup>20</sup> and surface

**Received:** September 24, 2010

**Published:** February 14, 2011

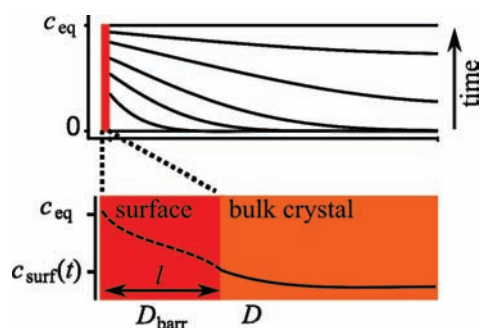


**Figure 1.** Conventional representation of a surface resistance as a thin layer of thickness  $l$  ( $\ll$  particle size  $L$ ) with a dramatically reduced diffusivity  $D_{\text{barr}}$  ( $\ll$  bulk diffusivity  $D$ ). The flux through the surface is driven by the difference between the equilibrium concentration  $c_{\text{eq}}$ , which is thought to be instantaneously attained on the outer side, and the concentration  $c(x=0) \equiv c_{\text{surf}}$  on the inner side of the surface layer. The concentration  $c_{\text{surf}} \equiv c(x=0)$  is the boundary value of the evolving concentration profiles in the interior of the particle (bulk phase) as observable by IFM and IRM.

permeabilities<sup>21</sup> in MOFs of type Zn(tbip) follow similar patterns of concentration and temperature dependence. An even more interesting finding is provided by considering the permeability/diffusivity ratio,  $\alpha/D$ . These ratios are calculated from the primary data (the surface permeabilities and intracrystalline diffusivities) as reported in refs 20 and 21 (crystals 1–3) and in this study (Figure 3, crystals 4 and 5) and are summarized in Table 1. Data evaluation and accuracy are detailed in section 3 of the Supporting Information. Remarkably, these calculations show that the permeability/diffusivity ratio  $\alpha/D$  of an individual crystal remains invariant with changes in (i) the type of the guest molecules, (ii) the loading (i.e., concentration of guest molecules), and (iii) the type of the diffusion process considered, i.e. transport diffusion (measured under nonequilibrium conditions) or self-(tracer) diffusion (under equilibrium conditions)!

In contrast to the conventional picture of transport resistances at phase boundaries as homogeneous layers of dramatically reduced diffusivities (or solubilities) with properties notably different from those of the bulk phase, surface permeation and intracrystalline diffusion in Zn(tbip) are evidently controlled by *the same* molecular mechanism! The experimental evidence therefore suggests that only a very small fraction of the pores are directly accessible from the outside atmosphere. After having passed these “entrances”, however, molecules are able to diffuse at the same rate as anywhere else within the pore space. Filling of the blocked pore channels may be accomplished via structural defects (“windows” between adjacent channels) which are known to occur even in seemingly ideal crystals.<sup>2,3</sup> This situation is illustrated by Figure 2.

In ref 22 the transient guest profiles during uptake and release in such structures are shown to coincide with the patterns for homogeneous resistances as shown in Figure 1. Examples of simulated profiles for subsequent times  $t_1 < t_2 < t_3$  are shown in Figure 2 and illustrated by possible particle distributions at these times. Note that now the quantity  $c(x=0)$  which appears in the definition (eq 1) of the surface barrier is the actual boundary concentration in the system. Assuming a statistical distribution of the channel openings (with probability  $p_{\text{open}}$ ) and of the “windows” between adjacent channels, i.e. in  $\pm y$  and  $\pm z$  directions (with probabilities  $p_y = p_z$ ), in ref 22 both simulations and probability estimates are shown to yield, as an analytical

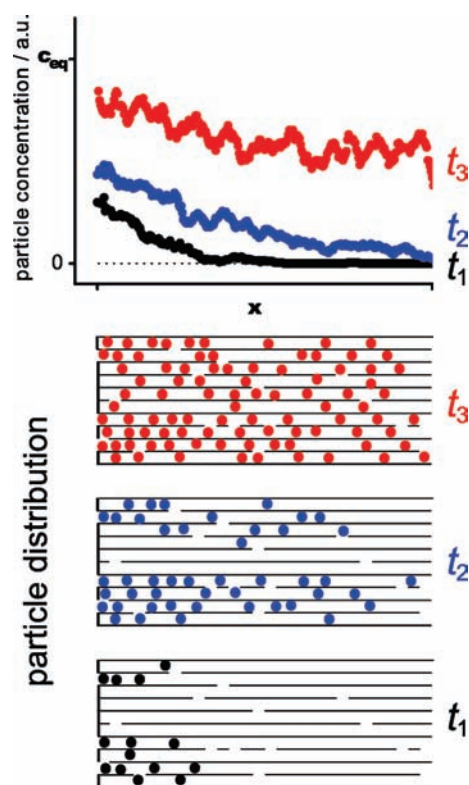


**Figure 2.** Schematics of the microstructural origin of surface resistances on nanoporous particles of type MOF-Zn(tbip): Entrances to most of the chains of cavities (“channels”) are blocked. Holes in the channel walls allow filling of all channels. Simulation results (top) show transient concentration profiles at times  $t_1 < t_2 < t_3$  during molecular uptake with examples of possible guest distributions (bottom).

expression:

$$\alpha \approx 0.5 \times \frac{p_{\text{open}} D}{\lambda} \frac{5p_y}{1 + 4p_y} \left( 1 - \frac{p_y}{2 + 4p_y} \right) \quad (4)$$

Here,  $\lambda$  denotes the simulation step length which, in the Zn(tbip) structure under consideration, coincides with the separation of adjacent cages (0.82 nm, see Supporting Figure 1). With eq 4 the permeability-to-diffusivity ratio  $\alpha/D$  is seen to be simply a function of the structural parameters of the given host material, which is exactly consistent with the results from our measurements. It is interesting to note that differences in the permeability/diffusivity ratios  $\alpha/D$  for different crystals (Table 1) result from differences in the surface permeability rather than from differences in the intracrystalline diffusivities. This finding agrees with the assumption that structural instabilities are likely to be much more pronounced close to the surface than in the crystal bulk phase.

Taking advantage of the arrangement of the cavities in one-dimensional chains (see Supporting Figure 1), the formalism of single-file diffusion<sup>23,24</sup> allows the rates of molecular uptake and release (or of tracer exchange) to be combined to estimate the probability that molecules are able to pass each other.<sup>22</sup> By attributing these mutual passages to structural defects in the system, one obtains  $p_y \approx 0.05$ . Inserting this value and  $\alpha/D = 0.6 \times 10^5$  as a typical value for the mean of the permeability/diffusivity ratios (Supporting Table 1), eq 4 yields  $p_{\text{open}} \approx 5 \times 10^{-4}$ . This result means that, on the average, within an area

Table 1. Surface Permeability/Diffusivity Ratio  $\alpha/D$  for Different Individual Crystals of Type Zn(tbip)

crystal	guest molecule	loading/molecules per segment	$D/10^{-13} \text{ m}^2 \text{ s}^{-1}$	$\alpha/10^{-8} \text{ m s}^{-1}$	ratio $\alpha/D/10^5 \text{ m}^{-1}$	
crystal 1	propane, 295 K	0	2.58	1.22	0.48	
		0.5	7.57	3.26	0.43	
		0.95	11.9	4.87	0.41	
	ethane, 295 K	0	484.56	139.52	0.29	
		0.5	1058.95	207.15	0.16	
		0.95	1.93	1.62	0.84	
	crystal 2	propane, 295 K	0	2.57	2.75	1.07
			0.5	7.57	5.94	0.79
			1	11.9	8.04	0.68
crystal 3 (tracer exchange)	propane, 295 K	0.28	1.18	0.38	0.32	
		0.47	0.63	0.21	0.33	
crystal 4	propane, 295 K	0	2.45	4.02	1.64	
		0.5	5.16	8.46	1.64	
		0.8	6.79	11.14	1.64	
	propane, 343 K	0	3.94	6.46	1.64	
		0.6	8.3	13.6	1.64	
		0.5	11.1	5.24	0.47	
crystal 5	propane, 295 K	0	2.45	1.15	0.47	
		0.5	5.16	2.42	0.47	
		0.8	6.79	3.19	0.47	
	propane, 323 K	0	3.94	1.85	0.47	
		0.5	8.3	3.9	0.47	
		0.5	5.92	2.49	0.47	
	propane, 343 K	0	5.92	2.49	0.47	
		0.5	11.1	5.24	0.47	

of about  $45 \times 45$  channel entrances on the crystal surface, there is only one that is open. This estimate holds for a statistical distribution of open channel entrances. For clustered channel openings and a given surface permeability, the percentage of open channel entrances increases in proportion with the diameter of the clusters of open channels.<sup>22,25</sup>

Measurements at different temperatures can provide further confirmation of the suggested origin of surface barriers. Practical restrictions of the apparatus in which IRM and IFM measurements are performed has hitherto prohibited transient uptake and release experiments at different temperatures. With the recently improved experimental system (Supporting Figure 2) this limitation has now been overcome, and the measurement of transient concentration profiles is no longer limited to being done at room temperature.

The surface permeabilities and intracrystalline diffusivities deduced from these profiles (Supporting Figures 5 and 6) are displayed in Figure 3. As required by the proposed model, both quantities show identical temperature dependencies. The difference in the permeability/diffusivity ratios of the two crystals may again be taken as an indication of different patterns of the surface blockages, while the similarity of the Arrhenius slopes confirms that surface permeation and bulk diffusion proceed by identical elementary mechanisms.

From the experimental evidence of the diffusion and permeation studies with guest molecules in Zn(tbip), the mechanism of mass transfer through the surface of nanoporous materials is found to be quite different from the conventional picture of a surface barrier as a homogeneous layer of dramatically reduced permeability. The experimental evidence is further supported

by dynamic Monte Carlo simulations and a formal analytical treatment which yield estimates of the fraction of unblocked pore entrances.<sup>22</sup>

The resistance model detected in our studies may occur quite generally at any phase boundary. While in the conventional view (Figure 1) the local permeation rate anywhere on the boundary is constant, the new model (Figure 2) represents the opposite limiting case where, with the exception of a few unblocked entrances, all remaining pores are totally blocked. Pore mouth opening by appropriate postsynthesis treatment (e.g., etching) thus, not unexpectedly, appears as an important route to enhancing surface permeability.

This scenario exemplifies a situation which, in theoretical physics, is generally treated by so-called effective-medium approaches.<sup>25–27</sup> In fact, for the prediction of the resulting concentration profiles it is immaterial whether one considers the real situation, i.e. a discontinuous resistance as reflected by Figure 2 or a continuous surface layer (an “effective medium”) with the permeability provided by eq 4. Mere inspection of the evolution of the concentration profiles in a particular experiment provides no direct evidence that would distinguish between these two models. It was the remarkable agreement between the (surface) permeabilities and (bulk) diffusivities which, for the given system, allowed the prediction of a highly discontinuous resistance with many blocked and a few open pore entrances.

The relevance of this finding is not limited to this particular system. With the advent of novel techniques of structure analysis<sup>28–30</sup> intergrowths have been shown to be a common feature of zeolite crystals. Internal barriers which may be formed at the internal boundaries of such intergrowths, have been suggested

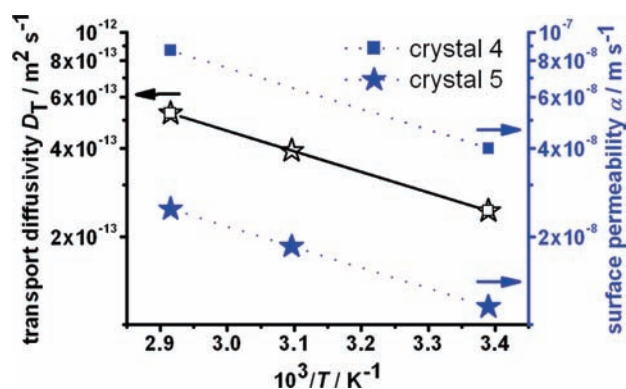


**Figure 3.** Temperature dependence of diffusivity and surface permeability. Surface permeability (filled symbols) and intracrystalline diffusivity (open symbols) of propane in MOF Zn(tbip) at vanishing loading at different temperatures, determined from the transient concentration profiles recorded in two different crystals during molecular uptake (Supporting Figures 5 and 6) by interference microscopy (IFM).

as a possible explanation of the discrepancy often observed on comparing macroscopic diffusion measurements (i.e., molecular uptake and release) with microscopic measurements.<sup>8,9,31</sup> If the microscopic measurements are made over diffusion path lengths notably smaller than the barrier separation, the measured diffusivity will not be affected by these resistances, which may, however, still control the overall rates of uptake and release. Though differing by orders of magnitude, the diffusivities determined in these two types of measurement often show similar patterns, including coinciding activation energies.<sup>8,9,31</sup> This remarkable finding from earlier comparative diffusion studies may now be easily explained if it is assumed that the internal barrier resistances are of the same type as the surface resistances observed in the present study.

In general, the nature of transport resistances may be expected to lie somewhere between the two limiting cases of a uniform low permeability (as has been widely assumed hitherto) and a highly heterogeneous permeability, varying between zero over most of the area and infinity for the “holes”, as observed in our present study. Recent advances in high-resolution microscopy and chemical analysis up to atomistic resolution,<sup>32</sup> in combination with microscopic diffusion studies, should provide the necessary tools to explore these more complicated structures, with the eventual goal of a complete understanding of the mechanisms leading to surface resistances and their consideration in the production of transport-optimized materials.

## ■ ASSOCIATED CONTENT

**Supporting Information.** Details on sample and experimental setup and data overview. This material is available free of charge via the Internet at <http://pubs.acs.org>.

## ■ AUTHOR INFORMATION

**Corresponding Author**  
kaerger@physik.uni-leipzig.de

## ■ ACKNOWLEDGMENT

We gratefully acknowledge the important contributions of Sergey Vasenkov, now at the University of Florida, Gainesville, and Pavel Kortunov, now at ExxonMobil, to the development of

our experimental device as well as financial support from the German Science Foundation, the Fonds der Chemischen Industrie, and the Alexander von Humboldt Foundation

## ■ REFERENCES

- (1) Corma, A.; Rey, F.; Rius, J.; Sabater, M. J.; Valencia, S. *Nature* **2004**, *431*, 287.
- (2) Agger, J. R.; Hanif, N.; Cundy, C. S.; Wade, A. P.; Dennison, S.; Rawlinson, P. A.; Anderson, M. W. *J. Am. Chem. Soc.* **2003**, *125*, 830.
- (3) Feldhoff, A.; Caro, J.; Jobic, H.; Olivier, J.; Krause, C. B.; Galvosas, P.; Kärger, J. *ChemPhysChem* **2009**, *10*, 2429.
- (4) Ruthven, D. M. In *Fundamentals of Adsorption Equilibrium and Kinetics in Microporous Solids*; Karge, H. G., Weitkamp, J., Eds.; Springer: Berlin, Heidelberg, 2008; Vol. 7, p 1.
- (5) Wloch, J. *Microporous Mesoporous Mater.* **2003**, *62*, 81.
- (6) Chmelik, C.; Varma, A.; Heinke, L.; Shah, D. B.; Kärger, J.; Kremer, F.; Wilczok, U.; Schmidt, W. *Chem. Mater.* **2007**, *19*, 6012.
- (7) Gobin, O. C.; Reitmeier, S. T.; Jentys, A.; Lercher, J. A. *Microporous Mesoporous Mater.* **2009**, *125*, 3.
- (8) Kärger, J.; Ruthven, D. M.; Theodorou, D. N.; Wiley-VCH: Weinheim, 2011.
- (9) Kärger, J.; Ruthven, D. M. *Diffusion in Zeolites and Other Microporous Solids*; Wiley & Sons: New York, 1992.
- (10) Bausinger, R.; Gersdorff, K. v.; Braekmans, K.; Ogris, M.; Wagner, E.; Bräuchle, C.; Zumbisch, A. *Angew. Chem., Int. Ed.* **2006**, *45*, 1568.
- (11) Chmelik, C.; Heinke, L.; Kortunov, P.; Li, J.; Olson, D.; Tzoulaki, D.; Weitkamp, J.; Kärger, J. *ChemPhysChem* **2009**, *10*, 2623.
- (12) Kärger, J.; Kortunov, P.; Vasenkov, S.; Heinke, L.; Shah, D. B.; Rakoczy, R. A.; Traa, Y.; Weitkamp, J. *Angew. Chem., Int. Ed.* **2006**, *45*, 7846.
- (13) Kortunov, P.; Heinke, L.; Arnold, M.; Nedellec, Y.; Jones, D. J.; Caro, J. *J. Am. Chem. Soc.* **2007**, *129*, 8041.
- (14) Tzoulaki, D.; Heinke, L.; Castro, M.; Cubillas, P.; Anderson, M. W.; Zhou, W.; Wright, P.; Kärger, J. *J. Am. Chem. Soc.* **2010**, *132*, 11665.
- (15) Pan, L.; Parker, B.; Huang, X.; Olson, D.; J.-Y., L.; Li, J. *J. Am. Chem. Soc.* **2006**, *128*, 4180.
- (16) Kocirik, M.; Struve, P.; Fiedler, K.; Bülow, M. *J. Chem. Soc., Faraday Trans. 1* **1988**, *84*, 3001.
- (17) Arya, G.; Maginn, E. J.; Chang, H. C. *J. Phys. Chem. B* **2001**, *105*, 2725.
- (18) Newsome, D. A.; Sholl, D. S. *J. Phys. Chem. B* **2005**, *2995*, 7237.
- (19) Crank, J. *The Mathematics of Diffusion*; Clarendon Press: Oxford, 1975.
- (20) Heinke, L.; Tzoulaki, D.; Chmelik, C.; Hibbe, F.; van Baten, J.; Lim, H.; Li, J.; Krishna, R.; Kärger, J. *Phys. Rev. Lett.* **2009**, *102*, 065901.
- (21) Tzoulaki, D.; Heinke, L.; Li, J.; Lim, H.; Olson, D.; Caro, J.; Krishna, R.; Chmelik, C.; Kärger, J. *Angew. Chem., Int. Ed.* **2009**, *48*, 3525.
- (22) Heinke, L.; Kärger, J. *Phys. Rev. Lett.* **2011**, *106*, 074501.
- (23) Hahn, K.; Kärger, J.; Kukla, V. *Phys. Rev. Lett.* **1996**, *76*, 2762.
- (24) Burada, P. S.; Hänggi, P.; Marchesoni, F.; Schmid, G.; Talkner, P. *ChemPhysChem* **2009**, *10*, 45.
- (25) Dudko, O. K.; Berezhkovskii, A. M.; Weiss, G. H. *J. Chem. Phys.* **2004**, *121*, 11283.
- (26) Tuck, C. *Effective Medium Theory*; Oxford University Press: Oxford, 1999.
- (27) Dudko, O. K.; Berezhkovskii, A. M.; Weiss, G. H. *J. Phys. Chem. B* **2005**, *109*, 21296.
- (28) Martinez, V. M.; de Cremer, G.; Roefiaers, M. B. J.; Sliwa, M.; Baruah, M.; de Vos, D. E.; Hofkens, J.; Sels, B. F. *J. Am. Chem. Soc.* **2008**, *130*, 13192.
- (29) Roefiaers, M. B. J.; Ameloot, R.; Baruah, M.; Uji-i, H.; Bulut, M.; de Cremer, G.; Muller, U.; Jacobs, P. A.; Hofkens, J.; Sels, B. F.; de Vos, D. E. *J. Am. Chem. Soc.* **2008**, *130*, 5763.
- (30) Weckhuysen, B. M. *Angew. Chem., Int. Ed.* **2009**, *48*, 4910.
- (31) Kärger, J.; Ruthven, D. M. *Zeolites* **1989**, *9*, 267.
- (32) Gross, L.; Mohn, F.; Moll, N.; Liljeroth, P.; Meyer, G. *Science* **2009**, *325*, 1110.